Reprinted from SPIE Vol. 819—Infrared Technology XIII

Invited Paper

Calibration and data reduction techniques for the AFGL astronomical infrared array spectrometer

Paul D. LeVan

Air Force Geophysics Laboratory
Hanscom AFB, Massachusetts 01731

Gregory Sloan

University of Wyoming, Department of Physics and Astronomy
Laramie, Wyoming 82071

ABSTRACT

Data reduction techniques have been implemented recently to obtain infrared spectra of astronomical objects from raw data obtained with the mosaic detector array and prism slit spectrometer used for groundbased telescope astronomical observations. During the course of the analysis, several instrumental peculiarities presented significant complications that were ultimately addressed. The techniques for flat fielding a slit spectrometer cannot follow exactly those used for an imaging camera, but a limited flat fielding approach can be used in conjunction with measurements of known calibration sources to calibrate the entire array. The end product described here allows a pipeline application of computer software to raw data frames that results in astronomical spectra independent of atmospheric and instrumental attenuation.

1. INTRODUCTION

The Air Force Geophysics Laboratory (AFGL) development of a transportable cryogenic dewar which encloses a Santa Barbara Research Center (SBRC) 58 by 62 Si:Ga mosaic array and prism slit spectrometer has resulted in its use on three separate occasions on the 92 inch telescope of the University of Wyoming, as described elsewhere[1]. Much current interest in the emerging widespread use of similar arrays, particularly at near-infrared wavelengths, is evidenced by recent conferences on the subject[1,2,3]. As a consequence of this activity, one would expect a corrresponding increase of publications relating to the data reduction techniques used to reduce the raw data with its instrumental dependencies into physically meaningful units.

The unwanted attributes of raw spectral data include the variations with wavelength of both atmospheric and instrumental transmission, and the separate night to night variations of atmospheric transmission. Dominating the 8 to 14 micron raw spectra gathered with the AFGL instrument is the 9.7 micron atmospheric ozone absorption which attenuates nearly 40% of the astronomical fluxes. Also important are the pixel responsivity variations both with wavelength and from pixel to pixel for a given wavelength. Working over a ten week period at AFGL, we have implemented computer code to eliminate these aspects of the raw data, producing the calibrated spectra required for analysis and publication in the astronomical and astrophysical literature. Because we are dealing with a slit spectrometer, which results in dispersion of the 8 to 14 micron spectrum along one axis of the array, flat fielding, or correction for pixel to pixel responsivity variations, cannot be accomplished solely with sky emission measurements at different zenith angles. On the other hand, it would be a difficult and error-prone process to cover all 58 spectral rows of the array with measurements of known astronomical calibration sources due to the difficulty of precisely centering the source on each of the rows. The optimal approach combines sky flat fielding for monochromatic pixel columns at wavelengths of high sky emissivity, e.g., the ozone band, with spectral calibrations at select spatial positions on the array using the bright astronomical standards. Data satisfying these requirements were gathered on one of the more recent observing runs, and reduction techniques using this data have led to reduced spectra which compare favorably with published spectra, in particular with the IRAS Low Resolution Spectrometer (LRS) spectra. The advantages of data gathered with a two-dimensional detector array employing a slit spectrometer over that obtained with a spectral scanning instrument of several discrete detectors are twofold. For use on a groundbased telescope, the slit spectrometer has the spectral multiplex advantage whereby all spectral elements are observed simultaneously, and the relative shape of the observed spectrum is less affected by variations in atmospheric transmission. Secondly, and important for either space or groundbased observations, each of the 62 wavelength channels of the slit spectrometer has spatial imaging capability over 58 spatial positions. This property is particularly advantageous if the infrared star is extended due to radiation from circumstellar dust, for which the spatial extent may vary with wavelength, or if the astronomical source contains ionized gas and dust, for which spatial variations of emission line

strengths would be indicative of either temperature or density morphology. For comparison with the LRS spectra, one may either take the peak spatial spectrum or the sum of the peak and sidelobe spectra obtained with the slit spectrometer.

2. CHARACTER OF THE RAW DATA

Because the background radiation levels from both the sky and telescope are so large in the ten micron region, an equal time is spent chopping between the astronomical source and an adjacent "blank sky" region. This large background also requires rapid and continuous scanning of the mosaic array during which the output signal from a given pixel is digitized and summed with the stored contents of the RAM address unique to that pixel. After scanning and storing for several tenths of a second, the address space is shifted to a separate block of RAM simultaneously with the movement of the telescope secondary mirror to the blank sky position (with electronic coaddition suppressed during the mirror settle time). This process can only be repeated several times before the 20 bit data bus approaches saturation, at which time the coadding terminates and the differences of the two RAM blocks are output for each pixel address to a minicomputer in a straight 16 bit binary format. Thus, the raw data from our observing runs consist of 58 by 62 pixel frames of digital data that result from electronically coadding into two separate RAM blocks individual 12 bit conversions up to 256 times, and subtracting these before storage onto a computer hard disk.

Gradients in atmospheric and telescope background levels between the two telescope chop positions are left as residuals after the differencing process, and can be a significant fraction of the astronomical source signal. Noise is present in the electronically coadded and differenced frame in the form of both spikes and additive electronics system noise. The single scanned frames of 12 bit conversions have an rms level of system noise at the second or third least significant bit, resulting in 50 to 100 noise counts after approximately 200 electronic coadds. The incidence of spikes is at the 10% level and is randomly distributed throughout electronically coadded frame. Frames of this type are gathered and stored repeatedly or hard disk during observations of single sources, and subsequent software coadding cannot proceed without compensation for the spikes discussed above, otherwise corruption of more than 50% of the coadded frame would result after only 7 coadds. Compensation of the above-mentioned issues will be discussed below.

3. DATA REDUCTION

We describe in the following subsections the sequence of processing steps in the order it is applied to the raw data frames.

3.1 Derivation of calibration coefficients.

The following outlines the procedure leading to flat field and spectral correction coefficients for each pixel in the array. Rows corresponding to point source spectra are independently corrected with measurements of an assumed point source standard star. The correction coefficients are the assumed standard star fluxes at the pixel wavelength divided by the output signal level for that pixel, and encompass both atmospheric and instrumental transmission variations with wavelength, as well as both the "average pixel" responsivity variation with wavelength and the pixel to pixel responsivity variations. Several row calibrations of this type averaged together represent the major correction for all other spectral rows in the mosaic array. An example of this "average spectral correction" derived from several rows of raw data for the bright infrared star IRC+10216 (see Figure 1) and the LRS spectrum for this object is shown in Figure 2. It is normalized to the fraction of pixels falling in the useable spectral range of the instrument. Variations for a given row from this average row

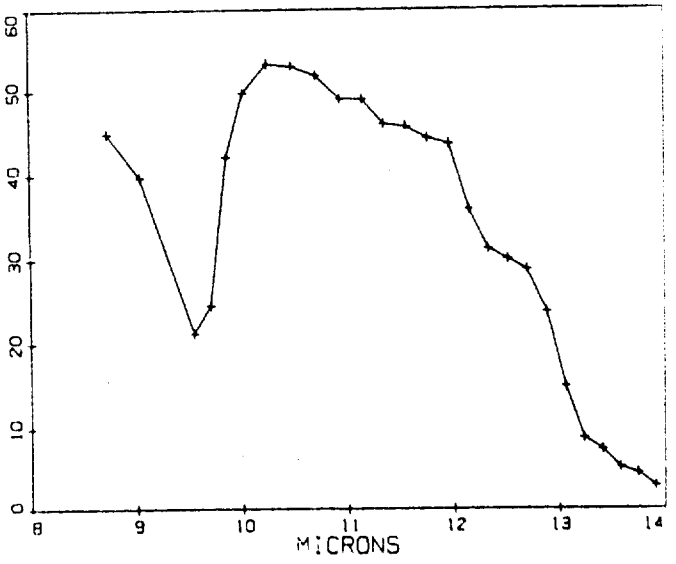

Figure 1. Raw spectral scan of the peak spatial row of the source IRC+10216.

SECURITY CLASSIFICATION OF THIS PAGE

ADA199141

REPORT DOCUMENTATION PAGE

1a. REPORT SECURITY CLASSIFICATION UNCLASSIFIED	1b. RESTRICTIVE MARKINGS
2a. SECURITY CLASSIFICATION AUTHORITY	3. DISTRIBUTION/AVAILABILITY OF REPORT Approved for public release; Distribution Unlimited
2b. DECLASSIFICATION/DOWNGRADING SCHEDULE	
4. PERFORMING ORGANIZATION REPORT NUMBER(S) AFGL-TR-88-0179	5. MONITORING ORGANIZATION REPORT NUMBER(S)
6a. NAME OF PERFORMING ORGANIZATION Air Force Geophysics Laboratory 6b. OFFICE SYMBOL (If applicable) OPC	7a. NAME OF MONITORING ORGANIZATION
6c. ADDRESS (City, State and ZIP Code) Hanscom AFB Massachusetts, 01731-5000	7b. ADDRESS (City, State and ZIP Code)
8a. NAME OF FUNDING/SPONSORING ORGANIZATION Air Force Office of Scientific Research 8b. OFFICE SYMBOL (If applicable) NP	9. PROCUREMENT INSTRUMENT IDENTIFICATION NUMBER
8c. ADDRESS (City, State and ZIP Code) BLDG 410 Bolling AFB, WA 20332	10. SOURCE OF FUNDING NOS. PROGRAM ELEMENT NO. 61102F; PROJECT NO. 2311; TASK NO. 2311G7; WORK UNIT NO. 01
11. TITLE (Include Security Classification) (U) Calibration and Data Reduction Techniques for the AFGL Astronomical IR Array Spectrometer	
12. PERSONAL AUTHOR(S) LeVAN PAUL D. and SLOAN, GREG, University of Wyoming	
13a. TYPE OF REPORT Reprint 13b. TIME COVERED FROM 86 OCT TO 87 SEP	14. DATE OF REPORT (Yr., Mo., Day) 1988 August 29 15. PAGE COUNT 6
16. SUPPLEMENTARY NOTATION Appeared in Proceeding of Society of Photo Optical Instrumentaion Engineers, Vol 819	

17. COSATI CODES		
FIELD	GROUP	SUB GR.
03	01	
03	02	

18. SUBJECT TERMS (Continue on reverse if necessary and identify by block number)
Infrared Spectrometers
Celestial Sources
Spectroscopy

19. ABSTRACT (Continue on reverse if necessary and identify by block number)

Data reduction techniques have been implemented recently to obtain infrared spectra of astronomical objects from raw data obtained with the mosaic detector array and prism slit spectrometer used for groundbased telescope astronomical observations. The techniques for flat fielding a slit spectrometer cannot follow exactly those used for an imaging camera, but a limited flat fielding approach can be used in conjunction with measurements of known calibration sources to calibrate the entire array. The end product described here allows a pipeline application of computer software to raw data frames that results in astronomical spectra independent of atmospheric and instrumental attenuation.

20. DISTRIBUTION/AVAILABILITY OF ABSTRACT UNCLASSIFIED/UNLIMITED ☒ SAME AS RPT. ☐ DTIC USERS ☐	21. ABSTRACT SECURITY CLASSIFICATION UNCLASSIFIED
22a. NAME OF RESPONSIBLE INDIVIDUAL PAUL D. LEVAN	22b. TELEPHONE NUMBER (Include Area Code) (617)377-4550 22c. OFFICE SYMBOL AFGL/OPC

DD FORM 1473, 83 APR EDITION OF 1 JAN 73 IS OBSOLETE.

SECURITY CLASSIFICATION OF THIS PAGE

correction are expressed as flat field correction factors that are nearly equal to unity for most all the array pixels away from the four edges. The standard star cannot be used to set the relative spatial response corrections unless an image blur functional form is assumed, and this is believed to be unreliable. However, relative row to row correction coefficients may be derived for a column of pixels using sky flat field techniques, because this column approximates a truely monochromatic linear array. We calculate these spatial correction coefficients for several columns in the atmospheric ozone band, any one of which could individually be used in conjunction with the spectral correction coefficients to set individual rows relative to each other. We flat field using dc sky measurements at zenith and at large (approximately 2 air mass) zenith angles. The difference in signal for the "ozone pixels" is sufficiently large to allow a 10% determination of these spatial correction coefficients from a single frame (5 msec integration time) of sky data. Because the mosaic array response has been shown to be linear in this regime, the subtracted value of signal counts at low and high air mass is proportional to the pixel responsivity, and equivalent to the slope of a linear fit. The spatial correction coefficients thus derived are used in conjunction with the average spectral correction and flat field correction coefficients to set the relative levels of all 3596 pixels in the mosaic detector array.

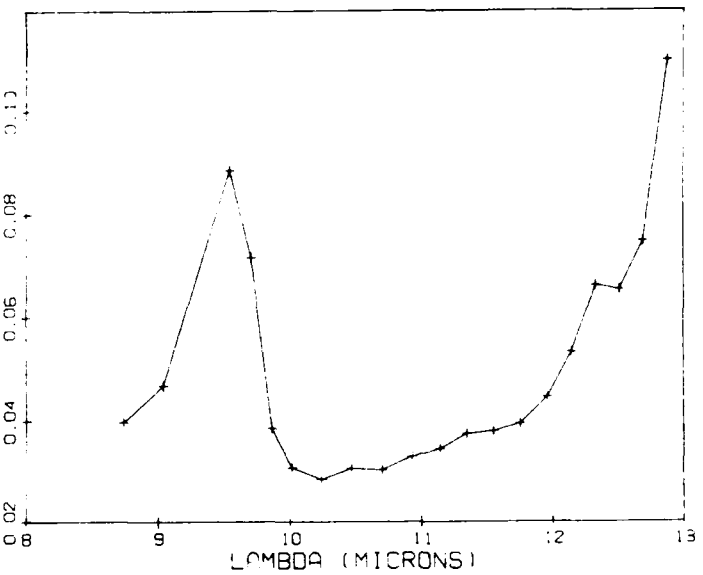

Figure 2. Average instrumental and atmospheric spectral correction.

3.2. Optical axis/mosaic array rotational misalignment.

The single significant complication to the above approach is presented by the approximate 1 degree misalignment of the mosaic array from the optical spectral and spatial principal axes. Applied without care, this approach leads to correction coefficients that exhibit a bifurcated structure about the peak row corresponding to the standard star position on the mosaic array. The correction coefficients have systematic positive slopes on one side of the peak source row and negative slopes on the other. These effects must be modelled and the associated trends removed, such that residual corrections are independent of position of the standard source on the array. Our confidence level in the above approach is bolstered by several tests. We apply the spectral correction coefficients to the standard star raw data (taken here as IRC + 10216 with the IRAS LRS spectrum as the assumed flux as a function of wavelength), and compare this with the assumed spectral distribution. In doing so, care must be taken because reduced program object spectra will also have spectral and spatial axes that deviate from the mosaic array row and column axes. (In the spatial case, the deviations are negligible over the limited extent of spatially-unresolved objects). These effects are discussed in the subsection below on optics misalignment compensation.

3.3 Spike identification.

Preprocessing of data in order to account for spiked pixels is necessary for objects fainter than IRC + 10216. The spikes are introduced at some point in the real-time digital signal processing, as repeat transfers of the RAM data to the minicomputer reproduce the spikes. We choose not to remove the spikes and re-estimate the true signal level but rather identify them and exclude them from subsequent processing. The identification process is a two stage one. The first stage is a two-point ratio test that tags points whose ratios exceed those corresponding with the spectral sampling interval across the instrumental response, if these points are also above the peak to peak noise range The second stage is a modified three point median filter, for which spike identification results if the midpoint exceeds in an absolute sense and by a threshold count value either of the two endpoints. Both stages are reset at the beginning of each spectral row, because there is no continuity of values expected between the end of one row and the beginning of the next. The combined stages identify as spikes approximately 10% of the total number of pixels in a frame electronically-coadded over a several second interval.

3.4 Software coaddition of the basic frames.

In order to increase integration time and thus the signal to noise for astronomical source observations, software coaddition of frames gathered in groups of ten is effectuated. The time for gathering several sets of frames in this way is sufficiently short to ignore effects of telescope track error and the longer time scale atmospheric seeing variations. Spikes identified as described above are clearly flagged for the steps which now follow. The software coadd routine sums defined pixel values and the squares of the defined values for each pixel into separate arrays. The number of defined values for each pixel over the course of the software coadd is tracked in a separate counter array. The three arrays that result after the desired number of coadds permit calculation of the average value and the standard deviation of the average value for each pixel, and the array of standard deviations is saved for subsequent analysis of the spectra in either graphic (see error bars in Figures 3 and 4) or numerical format.

3.5 Background residual subtraction.

For frames containing point astronomical sources the spatial extent due to atmospheric and diffraction effects is over only a few rows of the array, and the remaining spatial rows are purely background residuals. These "off-signal" rows can be used to estimate the subtracted component for the signal rows. A single background residual row applicable to all signal rows is formed by coadding as for frames, retaining the sum of defined values and the sum of the squares of these values in separate (linear) arrays. The number of defined values for each element in the row array is also stored, allowing calculation as for frame coadds of the average and its standard deviation for each pixel in the row. The noise due to random fluctuations obtained in this way will always be less than those for the signal rows taken separately, so subtraction from the signal rows will not raise significantly the noise. There are, however, errors in the background residual estimator due to the effects of responsivity variations along the columns of summed pixels, and this will dominate the random errors after an undetermined number of coadds. Since the pixel responsivity variations are well below 50% for most all pixels away from the array edges, the error incurred in the above approach will be a corresponding percentage of the average background residual value. Alternatively, the flat field coefficients could be applied to the coadded frame on a pixel by pixel basis before background residual subtraction, but this leads to an error because the signal rows are contaminated by the residuals at the time of the application.

3.6 Application of calibration coefficients.

The application of the average spectral correction to each signal row removes the atmospheric and instrumental transmission effects as well as the average pixel responsivity variation with wavelength (see Figures 3 and 4). The reductions of program objects result in reasonably good removal of the atmospheric ozone feature, which represents a compensation of more than a factor of two. This correction is followed by application of each pixel's flat field correction for all pixels in the signal rows. A minor correction proved necessary for the data set described here due to the fact that the calibration source was measured on a different night than the program objects. The start sequence of storage of mosaic array pixels in RAM locations is sensitive to the timing electronics settings, particularly the delay of the A to D convert pulse. The variable delay is directly related to the number of RAM addresses carried by the FIFO buffer. The pixels in a given row of RAM may thus be displaced by integer amounts from night to night, changing the wavelength calibration by a fixed amount for all rows. This effect was recognized after blindly applying the calibration coefficients which resulted in overcompensation of the atmospheric ozone off to one side of the peak and undercompensation on the other side, but was easily remedied by incorporating an integer shift in the application of correction coefficients to the program object data.

Finally, those rows requiring overall correction as evidenced by the sky emission flat fielding were addressed. After this, the relative pixel signal values reflect those of the astronomical source both spatially and spectrally, but will exhibit a skew relative to the orthogonal spatial and spectral axes due to the optics rotational misalignment. With this in mind, color temperature determinations for measured sources with LRS spectra result in favorable comparisons with the LRS colors, with both deviating from pure blackbody colors consistent with the presence of known broad emission features.

3.7 Compensation for optics misalignment.

The effects of the small value of rotational misalignment of the optical and mosaic array axes on the calibration coefficients determinations is discussed in the relevant subsection above. The misalignment manifests itself again in the reduced row spectra, such that rows above (North of) the peak row show red tilts of the overall spectral distribution whereas rows below (South of) the peak show blue tilts. Thus, individual

row spectra cannot be used for subsequent analysis. In order to correct this condition, one must consider "slices" oblique to the individual rows whose values are determined by combinations of bisected pairs of pixel values. The algorithm adopted here uses the known misalignment angle to calculate a rotated grid corresponding to the true spatial and spectral axes of the optics. Values on the rotated grid result from averaging old grid values within a fixed radius of the new grid point, weighted by the inverse of the distance between the old and new points. This results in row spectra over the spatial extent of the source that are somewhat smoothed relative to the original values but which taken individually describe the true energy distribution of the astronomical source. More details on this approach are contained in the final report[4] of Gregory Sloan prepared upon completion of his summer research at AFGL.

3.8 Wavelength calibration.

The remaining transformation to physical units is from pixel position in each row to wavelength. This wavelength calibration, or assignment of wavelengths, is determined by prism geometry (prism apex angle and angle of incidence of collimated beam), the refractive index as a function of wavelength for the prism material, and the camera mirror focal length. The camera mirror reimages the dispersed radiation onto the mosaic array and its focal length is the conversion from angular to linear dispersion. Five place accuracy values of the index of refraction of NaCl were taken from a compilation in the Handbook of Optics (W.G. Driscoll, ed., 1978). The prism equation for the deviation angle is solved as a function of wavelength corresponding to bins determined by the pixel spacings. A single pixel for which the wavelength is known a priori, based on its identification with the ozone absorption trough or, better, with a nebular emission line, provides a reference to which the remaining deviations are related. As a check, the calculated distance from the array edge of HeNe radiation (6328A) is compared with the room temperature value used in the original translational alignment of the optics to the mosaic array.

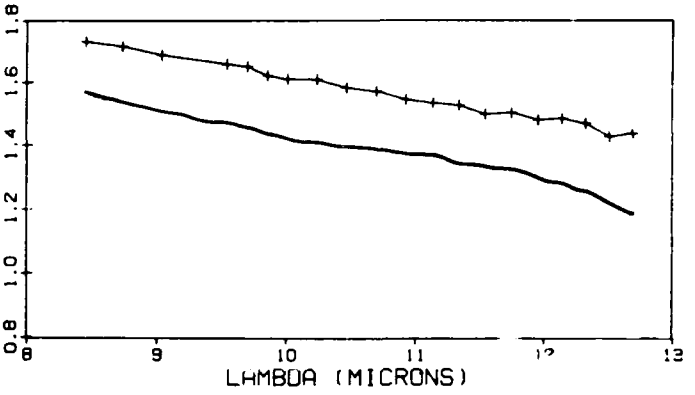

Figure 3. Mosaic array (top) and LRS (bottom) spectra for IRC+10216. Spectral flux (watt/m^2-micron) is plotted logarithmically and both curves have been shifted by arbitrary amounts.

3.9 Comparison with published results.

The LRS spectra for two infrared stars, IRC+10216 and Betelgeuse, are compared with the new slit spectrometer spectra reduced using the corrections outlined above and summing together the peak spatial and sidelobe spectra. Logarithmic values of relative spectral flux (watt/μm^2 micron) are plotted in order to allow overall shape comparisons. The results for IRC+10216 (Figure 3) are not surprising as the LRS spectrum for this object was used to derive the calibration coefficients, but the comparison is a valuable test of coaddition and optical misalignment correction techniques. For Betelgeuse (Figure 4), the shape of the LRS spectrum is also within the error bars of that for the slit spectrometer data. Variability of the relative spectral shape of IRC+10216 between the IRAS

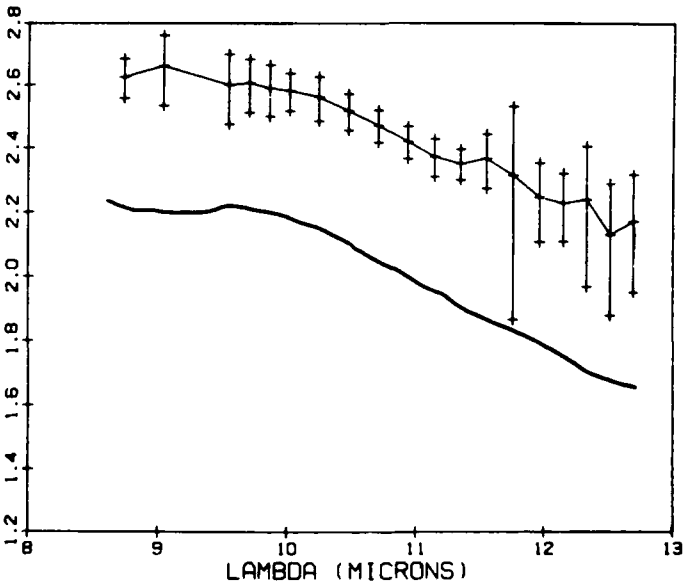

Figure 4. Mosaic array (top) and LRS (bottom) spectra for Betelegeuse. The plot is otherwise similar to Figure 3.

epoch (1983) and that of our observations (1987) cannot be dismissed as a possibility and should be borne in mind for the Figure 4 comparison.

4. FUTURE WORK

Several implications for calibration and program object observations during future observing runs are suggested by the present results. Spectral correction coefficients can be obtained for all 58 rows of the mosaic array by calibration star measurements over approximately 10 to 15 evenly spaced spatial positions due to the extent of the optics blur over several spatial elements. IRC+10216 is the logical choice for this because it allows high signal to noise determinations of the coefficients over short electronically-coadded exposures. However, because of possible temporal variation in the relative spectral shape of this object, it will be necessary to supplement the set of measurements at the various spatial positions with measurements at one spatial position of a (fainter) non-variable calibration source, for which a relative spectral shape will be assumed, using many software coadds. Cancellation of the residuals in the atmospheric and telescopic background subtraction will be effectuated using beam switching. Beam switching is a well-known technique whereby the telescope pointing direction is changed by an amount equal to the secondary mirror chop amplitude, such that the blank sky field is switched from north to south of the astronomical source. Performing this operation after sets of ten or more electronically-coadded frames will subtract the residual and not appreciably lower the observing efficiency. Finally, the spike identification algorithms will be adapted for use at the observing site so that software coaddition of electronically-coadded frames may be performed. This will dramatically decrease the hard disk data storage requirements which were faced on previous observing runs.

5. ACKNOWLEDGEMENTS

This work was supported by an Air Force Office of Scientific Research (AFOSR) task implemented at AFGL, and the support of the AFOSR is gratefully acknowledged. Individuals at AFGL who were indispensable include Peter Tandy and Leonard Marcotte. Don Campbell and Jack Carlin at SBRC provided support resulting in the loan of the infrared mosaic array. RDP, Inc., is acknowledged for display software developed under a prior AFGL contract. Dr. LeVan is grateful to J. Benson, T. Hayward, and K. Klett for aid in gathering the observational data.

6. REFERENCES

1. LeVan, P.D. and Tandy, P.C., "Recent Astronomical Results Obtained with the AFGL Ten Micron Array Spectrometer", in Workshop on Ground-based Astronomical Observations with IR Array Detectors, University of Hawaii, Hilo, Hawaii, 1987.

2. Wyoming Infrared Observatory Conference on IR Detector Arrays, University of Wyoming, Laramie, Wyoming, 1983.

3. Proceedings of the Second Infrared Detector Technology Workshop, C.R. McCreight, ed., NASA Tech. Memo. 88213, 1985.

4. Sloan, G., "Calibration and Data Reduction Techniques for the AFGL IR Array Spectrometer", final report submitted to Universal Energy Systems, Inc., upon completion of the Air Force Office of Scientific Research Graduate Student Summer Support Program, 1987.